

1 **Title: Components of Isolated Skeletal Muscle Differentiated Through Antibody Validation**

2 **Authors and Affiliations:** Dominique C. Stephens^{1,2*}, Margaret Mungai^{3*}, Amber Crabtree^{1*},
3 Heather K. Beasley¹, Edgar Garza-Lopez³, Larry Vang¹, Kit Neikirk¹, Zer Vue¹, Neng Vue¹,
4 Andrea G. Marshall¹, Kyrin Turner², Jian-qiang Shao⁴, Bishnu Sarker⁵, Sandra Murray⁶, Jennifer
5 A. Gaddy^{7,8}, Jamaine Davis⁹, Steven M. Damo^{2#}, Antentor O. Hinton Jr^{1#}

6 1. Department of Molecular Physiology and Biophysics, Vanderbilt University, Nashville, TN,
7 37232, USA

8 2. Department of Life and Physical Sciences, Fisk University, Nashville, TN, 37232, USA

9 3. Department of Internal Medicine, University of Iowa, Iowa City, IA, 52242, USA

10 4. Central Microscopy Research Facility, University of Iowa, Iowa City, IA, 52242, USA

11 5. School of Applied Computational Sciences, Meharry Medical College, Nashville, TN, 37232,
12 USA

13 6. Department of Cell Biology, College of Medicine, University of Pittsburgh, Pittsburgh, TN,
14 15260, USA

15 7. Division of Infectious Diseases, Vanderbilt University School of Medicine, Nashville,
16 Tennessee, USA

17 8. Tennessee Valley Healthcare Systems, U.S. Department of Veterans Affairs, Nashville,
18 Tennessee, USA

19 9. Department of Biochemistry and Cancer Biology. Meharry Medical College, Nashville, TN,
20 USA

21

22 *Co-first Authors

23 #Corresponding Authors:

24 Steven Damo, PhD

25 Fisk University

26 sdamo@fisk.edu

27

28 Antentor O. Hinton, Jr, PhD

29 Vanderbilt School of Medicine Basic Sciences

30 antentor.o.hinton.jr@Vanderbilt.edu

31

32

33

34 **Abstract**

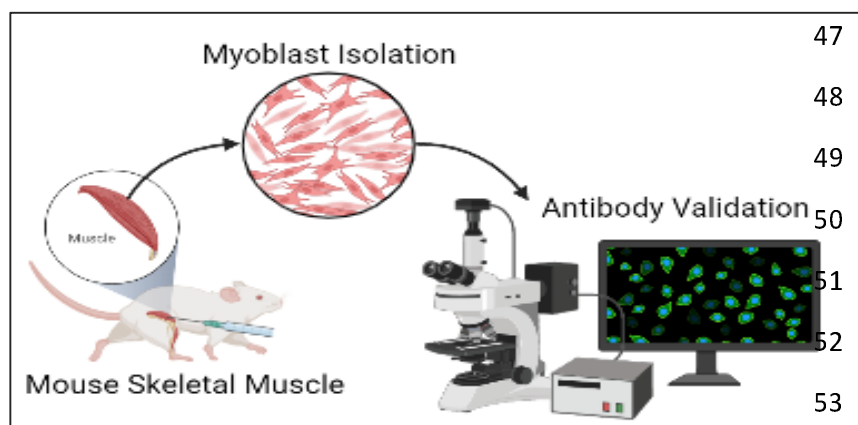
35 Isolation of skeletal muscles allows for the exploration of many complex diseases. Fibroblasts
36 and myoblast play important roles in skeletal muscle morphology and function. However,
37 skeletal muscles are complex and made up of many cellular populations and validation of these
38 populations is highly important. Therefore, in this article, we discuss a comprehensive method to
39 isolate mice skeletal muscle, create satellite cells for tissue culture, and use immunofluorescence
40 to validate our approach.

41 Novel imaging technology is increasing our ability to visualize and analyze cellular organelles
42 and compartments.

43 **Tweetable Abstract**

44 Proper antibody validation of cellular populations within isolated skeletal muscle can lead to
45 better elucidation of skeletal muscle structure and function, and their roles in complex diseases.

46 **Graphical Abstract**



54

55 **Method Summary**

56 Myoblasts are isolated from mouse limb muscles. They are plated for immunofluorescence-based
57 validation using confocal microscopy. This method demonstrates the need for reliable antibodies
58 to correctly determine and differentiate between cellular populations within isolated skeletal
59 muscles.

60 **Keywords:** Skeletal muscles, antibody validation, myoblast, fibroblast, immunofluorescence

61

62 **Introduction**

63 Skeletal muscles allow for animals and humans to be mobile ¹. Defects in skeletal muscle
64 (SkM) mass can cause atrophy and other pathological diseases ². Since the first description of
65 skeletal muscle diseases ³, there have been numerous discoveries describing their pathology and
66 the next step in studying these pathologies is characterizing the different cellular populations
67 residing within them. Isolating cells from these muscles allows for models to develop more
68 complex studies to understand how these pathological mechanisms work. In addition to muscle
69 diseases, skeletal muscles are also used to study immunological, neuronal, and other chronic
70 diseases ⁴. Specifically, skeletal muscle cells are essential for studies on exercise and insulin
71 stimulation. They are also useful experimental model to answer more complex questions, such as
72 the effects of insulin stimulation ⁵ on organelle morphology and the efficacy of new microscopy
73 methods like Focused Ion Beam Scanning Electron Microscopy (FIB-SEM) ⁶.

74 Here we offer two aims, firstly to show how to develop isolate myoblasts, or
75 differentiated myotubes, from murine skeletal muscle (**Figure 1**). Secondly, developing
76 antibody-based approaches for validating SkM cells has been a challenge. Here we also offer a
77 technique for myoblast validation.

78 Antibodies are useful for validating different populations of skeletal muscle cells.
79 Antibodies allow researchers to study the diversity of muscle fibers and cells while providing
80 important insights into cellular processes and disease development. Here, we listed common
81 antibodies used to study different cell populations in SkM tissue (**Table 1**).

82 SkM tissue is composed of various cell types with different functions, including
83 myoblasts and fibroblasts ². Skeletal myoblasts drive muscle regeneration after injury, while
84 fibroblasts create extracellular matrix components and secrete growth factors ⁷ (**Figure 2**).
85 Morphologically, fibroblasts are larger than myoblasts and contain more vesicles ⁸. Given that
86 these populations have morphological differences ⁹, validating that myoblast or myotube
87 differentiation is successful is of critical importance, especially for experiments that seek to
88 study homogenous populations and fine ultrastructural changes. Antibodies and fluorescence
89 light microscopy can be used to validate different cell populations in skeletal muscle tissue
90 (**Figure 3A-D**). Together, here we propose a standardized approach to isolate and identify
91 different skeletal muscle cell populations.

92

93 **Before you Begin:**

94

95 Initial PBS Wash mixture:

Name	Volume
PBS	25 mL
Fungizone	75 μ L
Penicillin-Streptomycin	250 μ L

96

97 Initial DMEM-F12 incubation mixture:

Name	Volume
DMEM-F12	250 mL DMEM (+ 4.5 g/L D-glucose, + L-Glut, -

	Sodium Pyruvate) + 250 mL F-12 (+L-Glut)
Collagenase II	1300 mg
Penicillin-Streptomycin	6.4 mL
Fungizone	2.0 mL

98

99

100 Secondary DMEM-F12 incubation mixture:

Name	Volume
DMEM-F12	250 mL DMEM (+ 4.5 g/L D-glucose, + L-Glut, - Sodium Pyruvate) + 250 mL F-12 (+L-Glut)
Collagenase II	650 mg
Penicillin-Streptomycin	6.4 mL
Fungizone	2.0 mL
Dipase	325 mg

101

102 DMEM-F12 Growth Media:

103 Mix the following. Use a sterile filter with Millipore brand 0.22 μ M filter units. Store at 4C for
 104 no longer than 2 months. Add bFGF (10ng/mL) to the aliquot just before adding it to plate.

Name	Volume	Example Catalog
DMEM-F12	250 mL DMEM (+ 4.5 g/L D-glucose, + L-Glut, - Sodium Pyruvate) + 250 mL F-12 (+L-Glut)	Gibco 11965-092 Gibco 11765-054
FBS	129 mL	Atlanta Biologicals S11550
Note: Do not heat inactivate FBS. Just thaw, swirl to mix, and go.		
Penicillin-Streptomycin	6.4 mL	Gibco 15140
Fungizone	2.0 mL	Gibco 15290-018
MEM Non-essential Amino Acids	6.4 mL	Gibco 11140

Beta-Mercaptoethanol	6.4 μ L	Gibco 21985-023

105

106

107 Permeabilization Buffer:

Name	Volume
PBS	495.5 mL
Triton X-100	0.5 mL

108

109

110 Differentiation medium:

Name	Volume
DMEM (+ 4.5 g/L D-glucose, + L-Glut, - Sodium Pyruvate)	250 mL
F-12 (+L-Glut)	250 mL
FBS	10.5 mL
Note: Do not heat inactivate FBS. Just thaw, swirl to mix, and go.	
Insulin-transferrin-selenium-X (100x)	5.3 mL

111

112 Reconstitute Human FGF-basic (FGF-2/bFGF) Recombinant Protein (here we use ThermoFisher
113 13256-029). Briefly, to prepare a stock solution of bFGF at a concentration of 0.1 mg/mL,
114 reconstitute it in 100 μ L of 10 mM Tris (pH 7.6). Dilute in buffer containing 0.1% BSA and
115 store in polypropylene vials for up to six months at -20°C. Avoid freezing and rethawing.

116

117 **Guide:**

118 *Myoblast Isolation*

- 119 1. Collect muscle tissue from the gastrocnemius, quadriceps, and hamstring muscles at 4-8
120 weeks of age from mice.
- 121 2. Wash Isolated tissue 2-3 times with Initial PBS Wash Mixture.

122

123 **NOTE:** The PBS solution is prepared right before dissecting the tissue.

- 124 3. Incubate muscle tissue in the initial DMEM-F12 incubation mixture.

125

126 **CRITICAL:** Avoid filtering the DMEM-F12 media containing collagenase, 1% pen/strep, and 3
127 $\mu\text{L}/\text{mL}$ Fungizone. This solution must be added cold to reduce temperature shock.

- 128 4. Maintain the muscle solution in a 37 °C water bath for 10-15 mins.
129 5. Shake at 220 rpm, for an overall time of 1.5 hrs.
130 6. After incubation, wash the tissue 3-4 times with PBS.
131 7. Incubate in warm the initial DMEM-F12 incubation mixture while the tissue is shaken for
132 30 mins in a 37 °C water bath.

133

134 **NOTE:** Solution has to be pre-warmed to 37°C to ensure efficient mixing of dispase and as the
135 muscles were at 37°C after incubation

- 136 8. After shaking, ground tissue with mortar and pestle in the presence of liquid nitrogen.
137 9. Pass through a 100 μm , then 70 μm , cell strainer.
138 10. Centrifuge the solution at 1000 rpm for five mins to pellet the cells.
139 11. Transfer the to a plate and resuspended using DMEM-F12 growth media supplemented
140 with 40 ng/mL bFGF.
141 12. Pre-plate the cells for 1-3 hours on UNCOATED dishes to reduce the number of
142 fibroblasts.

143

144 **CRITICAL:** Fibroblasts can dilute satellite cells. Recommended for dystrophic or injured
145 muscle. Pre-plating on an uncoated plate causes fibroblasts to stick and be isolated. Fibroblasts
146 can separately be used to isolate and for other experiments.

- 147 13. Dilute cells 1:15 in PBS, then plate in a Matrigel-coated dish.

148

149 **NOTE:** To create Matrigel-coated dishes, dilute stock concentration (while keeping on ice) to
150 1:15 in sterile PBS in the hood. Put Matrigel solution on flask/plate, shake/tilt to coat the bottom,
151 incubate at room temperature in hood for 30 mins, and remove Matrigel solution back into its
152 original tube. Matrigel solution may be reused up to 5 times total.

- 153 14. Wait for activation, which takes 24-48 hrs, after which myoblasts will grow rapidly.
154 a. To maintain healthy myoblast cells, use the growth media supplemented with
155 bFGF (10 ng/mL).

156

157 **CRITICAL:** Use Differentiation Medium to go from myoblasts to myocytes and then to
158 myotubes (Figure 2).

159

- 160 15. Plate primary myoblast at $\sim 8 \times 10^6$ cells per well and to differentiate the cells, add
161 differentiation media, supplemented with 1:10,000 bFGF.

162

163 **NOTE:** This will depend on # of cell passages and type of treatment, adjust accordingly.

164 16. Incubate for 4 to 5 days.

165

166 **NOTE:** Switch out with fresh differentiation media every 2 days, supplemented with 1:10,000
167 bFGF.

168 17. Cells are split using accutase.

169

170 **Note: DO NOT** use trypsin to split the cells. Accutase is less harsh to the extracellular matrix,
171 surface proteins, and cytoskeleton of skeletal cells than trypsin, so it is highly preferred ¹⁰.

172 18. Cells are maintained in a hypoxic environment (5% O₂) at 37°C. If growing myotubes, A
173 confluency of 70-85% has to be reached prior to adding growth media.

174

175 *Myoblast Validation*

176 Immunofluorescence staining is effective for examining differences in skeletal muscles
177 simultaneously. Refer to Table 1 for a list of validated primary antibodies for skeletal muscles.
178 Select secondary antibodies that are compatible with the epifluorescence or confocal microscope
179 available to you.

180 **CRITICAL:** All steps are performed at room temperature unless otherwise indicated.

181 **NOTE:** This protocol for Immunofluorescence staining and antibody validation of isolated
182 skeletal muscle cells is an adaptation of Esper et al., skeletal muscle tissue immunofluorescence
183 labeling protocol ¹¹.

184 1. To prepare the cells for fluorescence microscopy, the cells fix them by incubating them in
185 4% PFA for five mins.

186 2. Wash three times for five mins using PBS.

187

188 **NOTE:** Ice-cold 100% methanol or acetone is an effective fixative for cryosections and more
189 suited for some antigens. Acetone is less harsh than methanol.

190 3. Incubate cells in permeabilization buffer for 10 mins.

191 4. Incubate cells in blocking solution for 1 hr at room temperature or overnight at 4 °C.

192

193 **NOTE:** When using permeabilization buffer, keep the solution away from the hydrophobic
194 barrier to avoid loss of hydrophobicity. If this happens, wash the slide well with PBS. Include
195 Mouse on Mouse (MOM) blocking reagent at a 1:40 dilution when staining mouse tissue with
196 antibodies raised in the mouse.

197 5. To begin immunostaining, dilute the primary and secondary antibodies in a blocking
198 solution according to the manufacturer's suggested ratio.

199

200 **NOTE:** It is acceptable to dilute antibodies in hybridoma supernatant when targeting multiple
201 antigens.

- 202 6. Aspirate the blocking buffer and cover the slide with the primary antibody solution.
- 203 7. Incubate the slides overnight at 4 °C.
- 204 8. On the following day, wash three times for five mins with PBS.
- 205 9. After washing, cover cells with secondary antibodies diluted in blocking buffer for 1 hr at
- 206 room temperature in the dark.

207

208 **NOTE:** Keep slides in the dark for the remainder of the protocol.

- 209 10. After incubation, wash the slides three times for five mins with PBS.
- 210 11. Incubate the cells with 1 µg/mL DAPI diluted in PBS for five mins.
- 211 12. Wash once with PBS for five min.
- 212 13. Aspirate the PBS and place 1–2 drops of mounting media on to the cells
- 213 14. Carefully place a coverslip on the slide, while avoiding air bubbles.
- 214 15. Let the slides dry in the dark for 1–2 hr before sealing the slides with clear nail polish.
- 215 16. Store the slides at 4 °C and image within 2 weeks.

216

217 **Expected Outcomes:**

218 Upon isolation of myoblast and myotube, we validated their structure in light microscopy
219 (Figure 3A). Furthermore, we viewed multinucleated myotubes through TEM to validate that
220 ultrastructure was as expected (Figure 3B). Transfection further showed myotubes demonstrated
221 fluorescence as expected (Figure 3C). From there, we performed staining for myosin and desmin,
222 muscle-specific proteins that play crucial roles in muscle cell structure and function¹², to
223 confirm that filaments were present as expected (Figure 3 D-D’’).

224 Once myoblasts and myotubes are validated, they can be used for a variety of studies
225 including to measure mitochondrial efficiency with oxygen consumption rate, western blot
226 analysis to look for expression of specific proteins in knockout studies, or a variety of electron
227 microscopy techniques such as serial block-face scanning-electron microscopy to perform 3D
228 reconstruction of organelles¹³ (Figure 4). As an example, to validate this method, we sought to
229 understand how insulin treatment (10 nM/L) in 2-hour increments may alter myoblast and
230 myotube function through the usage of a Seahorse XF96 analyzer, per past protocols¹⁴.

231 To begin with, time points 1-3 measure basal respiration, or baseline rate of oxygen
232 consumption by cells in culture without any treatment. Oligomycin (1 µg/ml) was added to
233 inhibit ATP synthase, which reduces mitochondrial respiration and leads to an increase in proton
234 gradient, to measure the amount of oxygen consumed by the myoblasts and myotubes to
235 maintain the proton gradient in time points 4-6. carbonyl cyanide 4-
236 (trifluoromethoxy)phenylhydrazone (FCCP; 1 µM) was then added in time points 7-9 which
237 allows electrons to flow freely through the chain for reserve capacity and maximum oxygen
238 consumption to be measured. Finally, rotenone (1 µM) and antimycin A (10 µM) were added in
239 time points 10-12 which inhibit electron transfer from NADH to ubiquinone and ubiquinol to
240 cytochrome c, respectively, to measure non-mitochondrial respiration¹⁵.

241 We found that for myoblasts, there is a significantly increased basal, maximum, and non-
242 mitochondrial OCR after 2 hours of insulin treatment, while this difference is retained or

243 exacerbated after 4 hours of insulin treatment (Figure 5A-B). After 6 hours of insulin treatment,
244 OCR conversely showed significant decreases in all of these parameters (Figure 5C). In
245 myotubes, after 2 and 4 hours of insulin treatment, we similarly noted a significant increase in
246 mitochondrial OCR (Figure 5D-E). Notably, the increase in basal, ATP-linked, maximum, and
247 non-mitochondrial OCR is much higher in 4 hours than 2 hours. Unlike myoblasts, 6 hours of
248 insulin treatment myotubes did not differ significantly from untreated cells (Figure 5F).
249 Importantly, there may be a differential response to insulin treatment in myoblasts and myotubes,
250 highlighting the importance of studying both models. This validated that the function of
251 myoblasts and myotubes are intact following this isolation.

252 From there we sought to elucidate if organelle proteins are affected following insulin
253 treatment and we targeted Optic atrophy protein 1 (OPA-1), which is a mitochondrial inner
254 membrane (IMM) fusion protein that mediates the fusion of the IMM between two mitochondria
255 while also serving roles in mitochondrial bioenergetics and cristae architecture¹⁷. OPA-1 is just
256 one of several proteins which modulate mitochondrial structure. For example, contrastingly,
257 Dynamin-related protein 1 (DRP-1) is a protein which initiates the fission process through
258 constriction of the mitochondria which divides the mitochondria into two separate organelles¹⁸.
259 However, given that OCR increased following insulin treatment, it is possible this is due to
260 increased mitochondrial area caused by upregulated mitochondrial fusion. To see if OPA-1 may
261 be changed in expression, we performed western blotting. When looking at OPA-1, we noticed a
262 significant continuous increase in protein levels in myoblasts across 2 and 4 hours of insulin
263 stimulation when normalized (Figure 6A-B). We further differentiated primary myotubes and
264 carried out these experiments again to see if any differences existed (Figure 6C-D). We noticed
265 significant increases in OPA-1 levels after 4 hours of insulin stimulation (Figure 6C-D).
266 Together, this suggests that insulin stimulation causes increased expression of OPA-1 in a short
267 time frame which is exacerbated in myotubes compared with myoblasts. These results are
268 suggestive that mitochondrial fusion may be a compensatory of insulin stimulation which occurs
269 through OPA-1-mediated mechanisms in myoblasts and myotubes. Together these data validate
270 this isolation and validation technique allows for the application of experimental models to
271 elucidate cellular processes.

272

273 **Quantification and Statistical Analysis:**

274 After differentiation, quantification can be done for many experimental designs. Here, we
275 performed seahorse analysis per prior methods¹⁴ with GraphPad Prism version 8.4.0 (GraphPad
276 Software, La Jolla, CA) was used to perform students' T-tests to measure statistical significance.

277 **Limitations:** This protocol has been optimized for mice gastrocnemius, quadriceps, and
278 hamstring muscles and may not be applicable to other model organisms or tissue types.
279 Compared with other protocols, ours takes a similar period of time¹⁹, but this can still be a slow
280 process that must be carried out across multiple days. While C2C12 myoblasts are ideal for this
281 protocol, increasingly human skeletal myoblasts are important to study and past protocols

282 indicate that differences in the procedure must be made, such as antisense miR-133a addition, to
283 promote the fast differentiation of human skeletal myoblasts²⁰.

284 **Trouble Shooting:**

285 **Problem:** Ultrastructure or Gross morphology of Myoblasts are Degraded

286 **Potential Solution:** This may be due to too much damage incurred to myoblasts during
287 preparation. Here, we found that tissue should first be digested with type II collagenase and
288 dispase, then ground by being put in liquid nitrogen with a mortar with a pestle, and finally
289 passed through cell strainers optimizes this procedure. However, reducing the time grounded or
290 reducing the amount of digestion can avoid potential damage to the myoblasts if it is occurring.

291 **Problem:** Contamination with Fibroblasts

292 **Potential Solution:** It is important to plate first on an uncoated plate. However, if fibroblasts are
293 still observed, pre-plating can be done twice. Antibody-based selection of fibroblast may cause
294 certain issues but can also be explored as an option to remove fibroblasts. If this remains an
295 issue, other methods have shown that using flowing cytometry can be used to identify and
296 remove fibroblasts²¹.

297 **Problem:** Low Cell Yield or Viability

298 **Potential Solution:** If myoblast or myotube viability is low increasing the concentration of
299 growth factors and assuming a sterile environment is attained is important. Reducing time with
300 accutase can also ensure cells are not treated too harshly.

301

302 **Resource Availability:**

303 *Lead contact*

304 Further information and requests for resources and reagents should be directed to and will be
305 fulfilled by the lead contact, Antentor Hinton (antentor.o.hinton.jr@Vanderbilt.Edu).

306

307 *Materials availability*

308 All generated materials, if applicable, are created in methods highlighted in the text above.

309

310 *Data and code availability*

311 Full data utilized and requests for data and code availability should be directed to and will be
312 fulfilled by the lead contact, Antentor Hinton (antentor.o.hinton.jr@Vanderbilt.Edu).

313

314

315 **Author Contributions**

316

317 **Acknowledgements**

318 All antibodies were obtained from the Iowa Developmental Studies Hybridoma Bank (DSHB).

319

320 **Financial & Competing Interests' Disclosure**

321 All authors have no competing interests.

322 This project was funded by the UNCF/Bristol-Myers Squibb E.E. Just Faculty Fund, BWF
323 Career Awards at the Scientific Interface Award, BWF Ad-hoc Award, NIH Small Research
324 Pilot Subaward to 5R25HL106365-12 from the National Institutes of Health PRIDE Program,
325 DK020593, Vanderbilt Diabetes and Research Training Center for DRTC Alzheimer's Disease
326 Pilot & Feasibility Program. CZI Science Diversity Leadership grant number 2022- 253529 from
327 the Chan Zuckerberg Initiative DAF, an advised fund of Silicon Valley Community Foundation
328 (to A.H.J.). NSF EES2112556, NSF EES1817282, and CZI Science Diversity Leadership grant
329 number 2022-253614 from the Chan Zuckerberg Initiative DAF, an advised fund of Silicon
330 Valley Community Foundation (to S.M. D.) and National Institutes of Health grant HD090061
331 and the Department of Veterans Affairs Office of Research award I01 BX005352 (to J.G.).
332 Additional support was provided by the Vanderbilt Institute for Clinical and Translational
333 Research program supported by the National Center for Research Resources, Grant UL1
334 RR024975-01, and the National Center for Advancing Translational Sciences, Grant 2 UL1
335 TR000445-06 and the Cell Imaging Shared Resource.

336

337 **Data Sharing and Open Access**

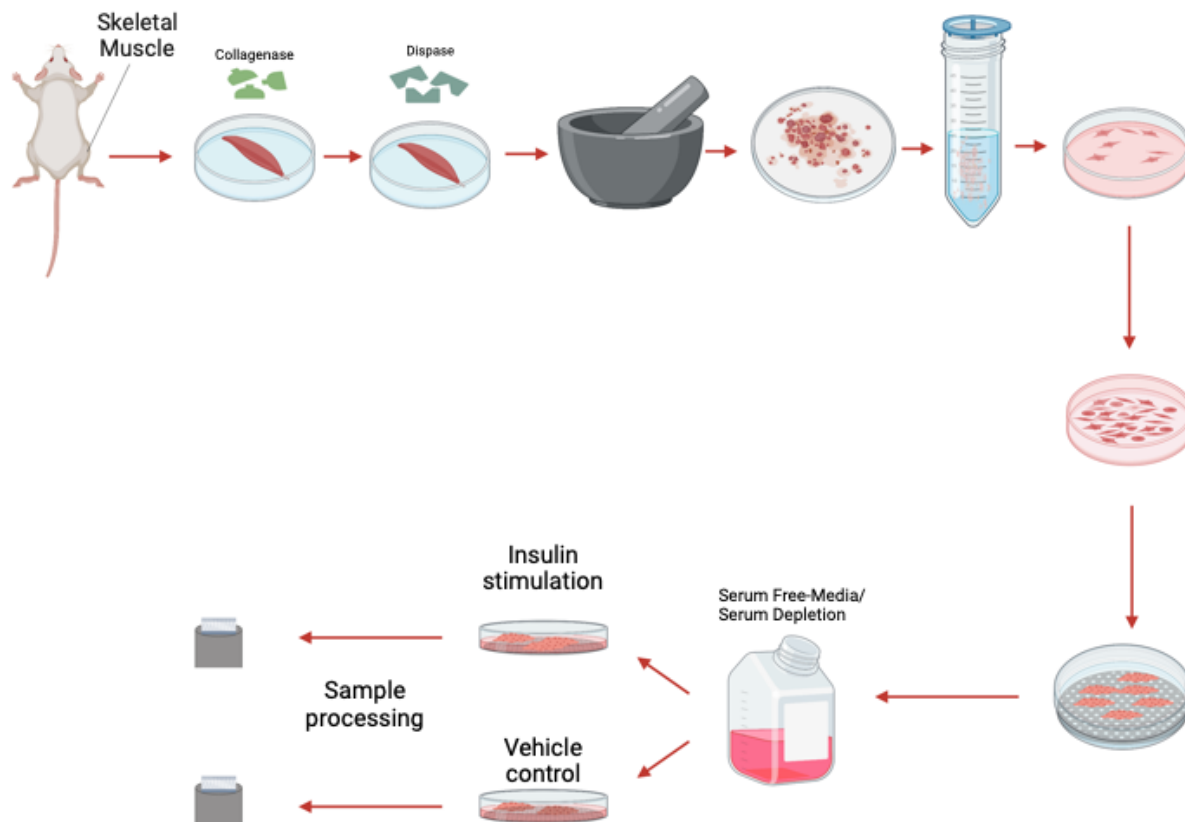
338 All data is available upon request to the corresponding author.

339

340

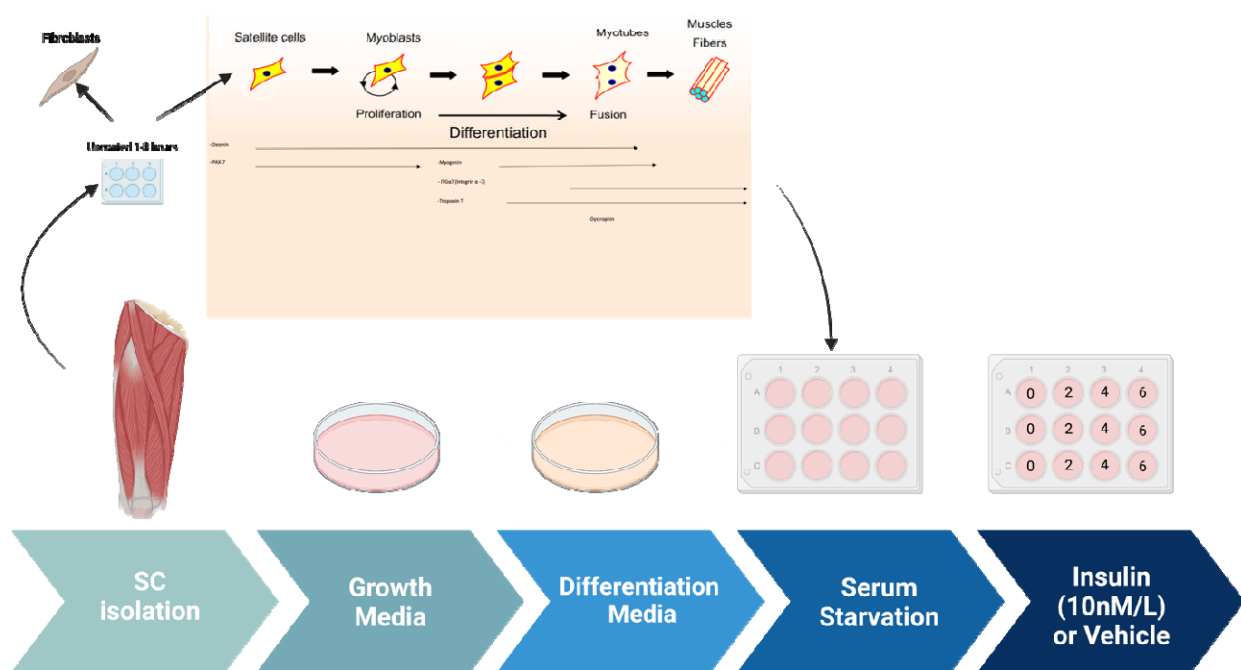
341 **Figures and Legends**

342



343

344 **Figure 1: The process of myoblast isolation from gastrocnemius muscle.**



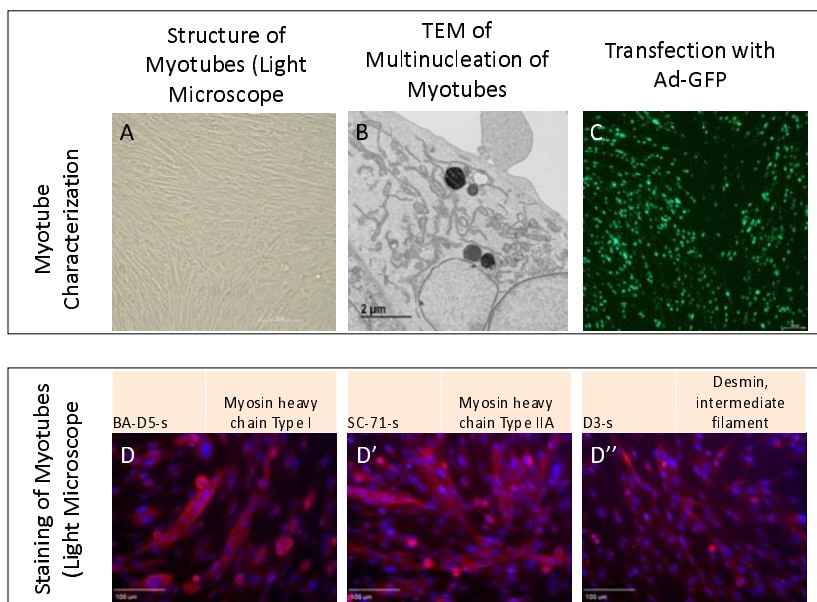
345

346 **Figure 2: The process of myotube differentiation from myoblasts and utilization for serum**

347

348

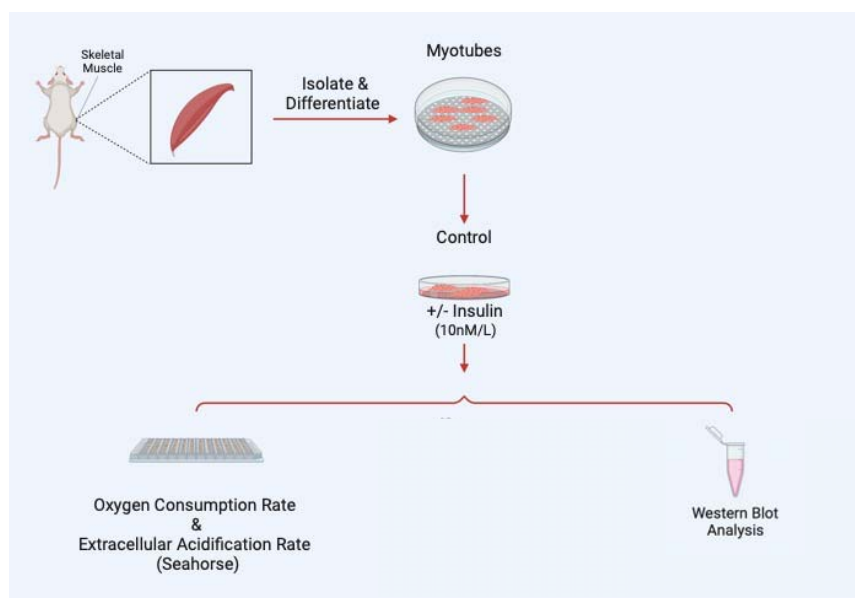
349



350

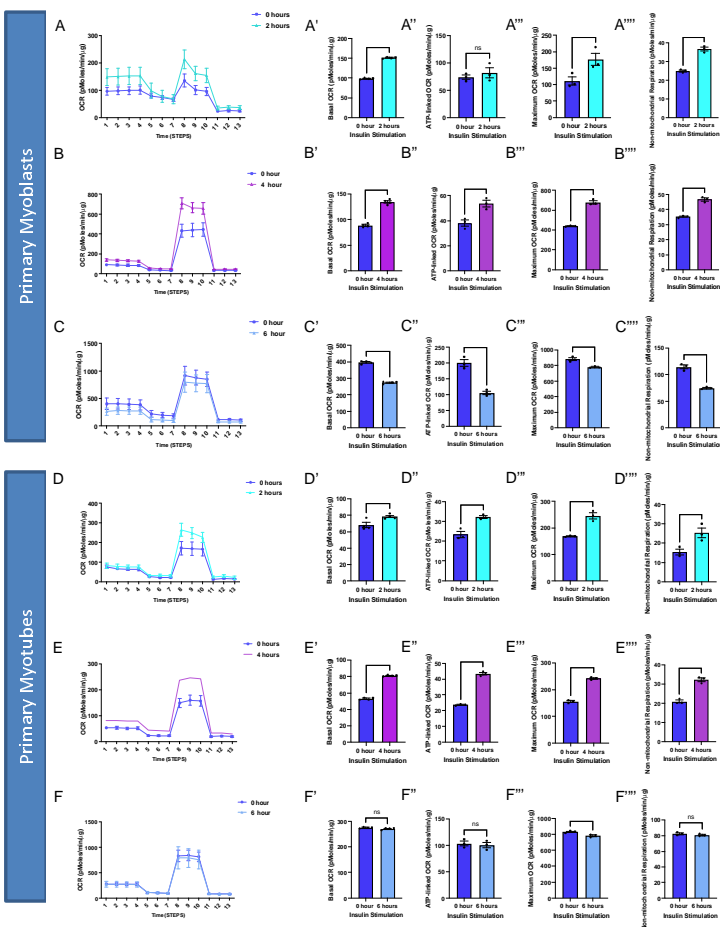
351 **Figure 3:** Myotubes as characterized by A. Light microscopy, B. Transmission electron
352 microscopy, and C. Transfection with adenovirus containing the green fluorescent protein gene
353 (Ad-GFP). D. Straining with BA-D5-s, D' SC-71-s, and D'' D3-s to show myosin and desmin.

354



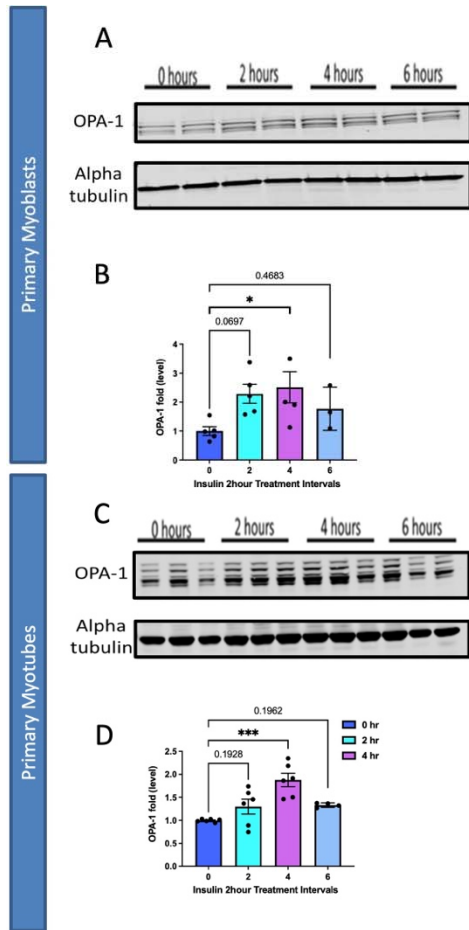
355

356 **Figure 4:** Examples of experiments that may be performed following myotube differentiation
357 and isolation.



358

359 **Figure 5:** Oxygen consumption rate (OCR) altered in myoblasts and myotubes upon altered
 360 insulin stimulation which shows changes in mitochondrial efficiency. (A) Seahorse plot for
 361 primary myoblasts following 2 hours of insulin stimulation (B) 4 hours of insulin stimulation and
 362 (C) 6 hours of insulin stimulation. (D) Oxygen consumption rate was measured after several
 363 inhibitors to measure respiration in primary myotubes after 2 hours, (E) 4 hours and (F) 6 hours
 364 of insulin stimulation. (A'-F') Basal OCR which represents respiration under normal, unstressed
 365 conditions. (A''-F'') ATP-linked OCR, which is respiration associated with ATP synthesis
 366 during oxidative phosphorylation which is marked by a reduction in OCR due to oligomycin.
 367 (A'''-F''') Maximum OCR which is the maximal capacity at which mitochondria may utilize
 368 oxygen. (A''''-F''''') Non-mitochondrial respiration which can be attributed to factors such as
 369 glycolysis or ROS and not due to mitochondrial respiration. These values were compared to the
 370 control (blue) in all of these examples. N = 6 per treatment, and * indicates p-value < .05.



371

372 **Figure 6:** Comparison of mitochondrial fusion proteins following insulin stimulation in primary
 373 myoblasts and myotubes. (A) Western blotting for mitochondrial fusion protein OPA-1
 374 following 2 hours, 4 hours, and 6 hours of insulin stimulation. (B) OPA-1 levels normalized to
 375 Alpha tubulin following insulin stimulation. (C) This was replicated in primary myotubes, as
 376 western blotting for mitochondrial fusion OPA1. (D) OPA-1 levels, normalized to Alpha tubulin,
 377 in primary myotubes following insulin treatment. N = 6 per treatment, and * indicates p-value <

378 .05.

Antibody Name	Antigen	IF/IB conc
BF-F3-s	Myosin heavy chain Type IIB	2-5 ug/ml 380
SC-71-s	Myosin heavy chain Type IIA	2-5 ug/ml 381
BA D5-s	Myosin heavy chain Type I	2-5 ug/ml 382
F5D-s	Myogenin	2-5 ug/ml 383
PAX7-s	Pax7	2.5 ug/ml 384
D3-s	Desmin, intermediate filament	2.5 ug/ml 385
9.1 ITGA7-s	Integrin alpha-7, extracellular domain	2-5 ug/ml 386
JLT12-s	troponin T, fast skeletal muscle specific	2.5 ug/ml

387

388

389

390

391

392

393 **Table 1:** A list of antibodies and their respective antigens for skeletal muscle validation after
394 isolation. The list was obtained from <https://dshb.biology.uiowa.edu/>.

395

396

397

398

399

400

401

402

403

404

405

406

407

408

409 **References**

- 410 1. Figueiredo, P.A., Mota, M.P., Appell, H.J., and Duarte, J.A. (2008). The role of
411 mitochondria in aging of skeletal muscle. *Biogerontology* 9, 67–84. [10.1007/s10522-007-](https://doi.org/10.1007/s10522-007-9121-7)
412 [9121-7](https://doi.org/10.1007/s10522-007-9121-7).
- 413 2. Dave, H.D., Shook, M., and Varacallo, M. (2022). Anatomy, Skeletal Muscle. In StatPearls
414 [Internet] (StatPearls Publishing).
- 415 3. Walusinski, O. (2022). François-Amilcar Aran (1817-1861) and the recognition of spinal
416 muscular atrophy. *Rev Neurol (Paris)* 178, 756–765. [10.1016/j.neurol.2022.01.011](https://doi.org/10.1016/j.neurol.2022.01.011).

- 417 4. Morgan, J., and Partridge, T. (2020). Skeletal muscle in health and disease. *Disease Models*
418 & *Mechanisms* *13*, dmm042192. 10.1242/dmm.042192.
- 419 5. Alonge, K.M., Meares, G.P., and Hillgartner, F.B. (2017). Glucagon and Insulin
420 Cooperatively Stimulate Fibroblast Growth Factor 21 Gene Transcription by Increasing the
421 Expression of Activating Transcription Factor 4 *. *Journal of Biological Chemistry* *292*,
422 5239–5252. 10.1074/jbc.M116.762922.
- 423 6. Marshall, A.G., Damo, S.A., and Hinton, A. (2023). Revisiting focused ion beam scanning
424 electron microscopy. *Trends Biochem Sci*, S0968-0004(23)00056-7.
425 10.1016/j.tibs.2023.02.005.
- 426 7. Thummarati, P., and Kino-Oka, M. (2020). Effect of Co-culturing Fibroblasts in Human
427 Skeletal Muscle Cell Sheet on Angiogenic Cytokine Balance and Angiogenesis. *Front*
428 *Bioeng Biotechnol* *8*, 578140. 10.3389/fbioe.2020.578140.
- 429 8. Yablonka-Reuveni, Z., Anderson, S.K., Bowen-Pope, D.F., and Nameroff, M. (1988).
430 Biochemical and morphological differences between fibroblasts and myoblasts from
431 embryonic chicken skeletal muscle. *Cell Tissue Res* *252*, 339–348. 10.1007/BF00214376.
- 432 9. Minguetti, G., and Mair, W.G. (1980). The developing human muscle: ultrastructural
433 differences between myoblasts and fibroblasts. *Rev Bras Pesqui Med Biol* *13*, 1–8.
- 434 10. Nowak-Terpiłowska, A., Śledziński, P., and Zeyland, J. (2021). Impact of cell harvesting
435 methods on detection of cell surface proteins and apoptotic markers. *Braz J Med Biol Res*
436 *54*, e10197. 10.1590/1414-431X202010197.
- 437 11. Esper, M.E., Kodippili, K., and Rudnicki, M.A. (2023). Immunofluorescence Labeling of
438 Skeletal Muscle in Development, Regeneration, and Disease. *Methods Mol Biol* *2566*, 113–
439 132. 10.1007/978-1-0716-2675-7_9.
- 440 12. Agnetti, G., Herrmann, H., and Cohen, S. (2022). New roles for desmin in the maintenance
441 of muscle homeostasis. *The FEBS Journal* *289*, 2755–2770. 10.1111/febs.15864.
- 442 13. Garza-Lopez, E., Vue, Z., Katti, P., Neikirk, K., Biete, M., Lam, J., Beasley, H.K., Marshall,
443 A.G., Rodman, T.A., Christensen, T.A., et al. (2022). Protocols for Generating Surfaces and
444 Measuring 3D Organelle Morphology Using Amira. *Cells* *11*, 65. 10.3390/cells11010065.
- 445 14. Pereira, R.O., Marti, A., Olvera, A.C., Tadinada, S.M., Bjorkman, S.H., Weatherford, E.T.,
446 Morgan, D.A., Westphal, M., Patel, P.H., and Kirby, A.K. (2021). OPA1 deletion in brown
447 adipose tissue improves thermoregulation and systemic metabolism via FGF21. *Elife* *10*,
448 e66519.
- 449 15. Rose, S., Frye, R., Slattery, J., Wynne, R., Tippet, M., Pavliv, O., Melnyk, S., and James, S.
450 (2014). Oxidative Stress Induces Mitochondrial Dysfunction in a Subset of Autism
451 Lymphoblastoid Cell Lines in a Well-Matched Case Control Cohort. *PLoS one* *9*, e85436.
452 10.1371/journal.pone.0085436.

- 453 16. Chen, H., Detmer, S.A., Ewald, A.J., Griffin, E.E., Fraser, S.E., and Chan, D.C. (2003).
454 Mitofusins Mfn1 and Mfn2 coordinately regulate mitochondrial fusion and are essential for
455 embryonic development. *J Cell Biol* 160, 189–200. 10.1083/jcb.200211046.
- 456 17. Barrera, M., Koob, S., Dikov, D., Vogel, F., and Reichert, A.S. (2016). OPA1 functionally
457 interacts with MIC60 but is dispensable for crista junction formation. *FEBS Letters* 590,
458 3309–3322. 10.1002/1873-3468.12384.
- 459 18. Peng, L., Men, X., Zhang, W., Wang, H., Xu, S., Xu, M., Xu, Y., Yang, W., and Lou, J.
460 (2011). Dynamin-related protein 1 is implicated in endoplasmic reticulum stress-induced
461 pancreatic β -cell apoptosis. *Int J Mol Med* 28, 161–169. 10.3892/ijmm.2011.684.
- 462 19. Shahini, A., Vydiam, K., Choudhury, D., Rajabian, N., Nguyen, T., Lei, P., and Andreadis,
463 S.T. (2018). Efficient and high yield isolation of myoblasts from skeletal muscle. *Stem Cell*
464 *Research* 30, 122–129. 10.1016/j.scr.2018.05.017.
- 465 20. Cheng, C.S., El-Abd, Y., Bui, K., Hyun, Y.-E., Hughes, R.H., Kraus, W.E., and Truskey,
466 G.A. (2014). Conditions that promote primary human skeletal myoblast culture and muscle
467 differentiation in vitro. *Am J Physiol Cell Physiol* 306, C385–C395.
468 10.1152/ajpcell.00179.2013.
- 469 21. Stellato, M., Czepiel, M., Distler, O., Błyszczuk, P., and Kania, G. (2019). Identification and
470 Isolation of Cardiac Fibroblasts From the Adult Mouse Heart Using Two-Color Flow
471 Cytometry. *Frontiers in Cardiovascular Medicine* 6.

472